Journal of Radiation Research, Vol. 59, No. 3, 2018, pp. 261–271
doi: 10.1093/jrr/rrx089
Advance Access Publication: 17 January 2018

Repair kinetics of DNA double-strand breaks and incidence of apoptosis in mouse neural stem/progenitor cells and their differentiated neurons exposed to ionizing radiation

Hiroki Kashiwagi[1,2], Kazunori Shiraishi[1], Kenta Sakaguchi[1], Tomoya Nakahama[1,3] and Seiji Kodama[1,*]

[1]Laboratory of Radiation Biology, Department of Biological Science, Graduate School of Science, Osaka Prefecture University, 1-2 Gakuen-cho, Naka-ku, Sakai, Osaka 599-8570, Japan
[2]National Institute of Occupational Safety and Health, Nagao 6-21-1, Tama-Ku, Kawasaki 214-8585, Japan
[3]Clinical Innovation, Sysmex Corporation, 4-4-4 Takatsukadai, Nishi-ku, Kobe 651-2271, Japan
*Corresponding author. Laboratory of Radiation Biology, Department of Biological Science, Graduate School of Science, Osaka Prefecture University, 1-2 Gakuen-cho, Naka-ku, Sakai, Osaka 599-8570, Japan. Tel. & Fax: +81-72-254-9855; Email: kodama@riast.osakafu-u.ac.jp
(Received 1 August 2017; revised 14 October 2017; editorial decision 8 December 2017)

ABSTRACT

Neuronal loss leads to neurodegenerative disorders, including Alzheimer's disease, Parkinson's disease and Huntington's disease. Because of their long lifespans, neurons are assumed to possess highly efficient DNA repair ability and to be able to protect themselves from deleterious DNA damage such as DNA double-strand breaks (DSBs) produced by intrinsic and extrinsic sources. However, it remains largely unknown whether the DSB repair ability of neurons is more efficient compared with that of other cells. Here, we investigated the repair kinetics of X-ray–induced DSBs in mouse neural cells by scoring the number of phosphorylated 53BP1 foci post irradiation. We found that p53-independent apoptosis was induced time dependently during differentiation from neural stem/progenitor cells (NSPCs) into neurons in culture for 48 h. DSB repair in neurons differentiated from NSPCs in culture was faster than that in mouse embryonic fibroblasts (MEFs), possibly due to the higher DNA-dependent protein kinase activity, but it was similar to that in NSPCs. Further, the incidence of p53-dependent apoptosis induced by X-irradiation in neurons was significantly higher than that in NSPCs. This difference in response of X-ray–induced apoptosis between neurons and NSPCs may reflect a difference in the fidelity of non-homologous end joining or a differential sensitivity to DNA damage other than DSBs.

Keywords: neural stem/progenitor cells (NSPCs); neurons; DNA double-strand breaks (DSBs); non-homologous end joining (NHEJ); DNA-dependent protein kinase (DNA-PK); apoptosis

INTRODUCTION

Maintenance of neurons throughout life is crucial because loss of neurons leads to neurodegenerative disorders, including Alzheimer's disease, Parkinson's disease and Huntington's disease [1]. DNA double-strand breaks (DSBs) are the type of DNA damage most likely to lead to cell death or genomic instability when they are unrepaired or misrepaired [2]. In fact, it is well known that DSBs accumulate in neurons of the model mice of Alzheimer's disease and Huntington's disease [3, 4], suggesting that DSBs contribute to neuronal loss. DSBs are generated by intrinsic sources such as reactive oxygen species (ROS), which in turn are generated by normal cellular metabolism, and extrinsic sources such as ionizing radiation [2]. Neurons can generate more ROS than other cells due to their high consumption of oxygen [5, 6]. In addition, DSBs are generated by physiological neuronal activity in mouse neurons [3, 7]. These facts suggest that the genome of neurons is always at risk of

DSBs under physiological brain activity. Additionally, neurons are differentiated from neural stem cells at an early stage of development and maintained throughout the life of the organisms, suggesting that neurons have efficient DSB repair. However, the ability of neurons to execute DSB repair remains largely undemonstrated.

In mammalian cells, DSBs are mainly repaired by non-homologous end joining (NHEJ) and homologous recombination (HR) [2, 8]. Although HR for DSB repair is limited to late S and G_2 phases, NHEJ is available at all phases of the cell cycle except the M phase, and thus NHEJ is the major DSB repair pathway in post-mitotic cells such as neurons [2]. The core proteins involved in NHEJ in mammalian cells are Ku70, Ku80, DNA-dependent protein kinase catalytic subunit (DNA-PKcs), Artemis, DNA ligase IV, XRCC4 and XLF/Cernunnos [2, 8]. Recently, PAXX (also known as XLS) has been identified as a new NHEJ component protein [9–11]. Moreover, mice expressing a kinase-dead DNA-PKcs [12], and targeted disruption of the genes encoding Ligase IV [13, 14] or XRCC4 [14] are embryonic lethal with neuronal apoptosis, suggesting that the components of NHEJ play an important role in developing and maintaining neurons.

For the present study, we adopted an *in vitro* cell differentiation system in which we could compare the DSB repair ability of neural stem cells and their differentiated neurons. We then investigated the relationship between DSB repair kinetics and the activity of DNA-dependent protein kinase (DNA-PK) (which plays a major role in NHEJ) in mouse neural stem/progenitor cells (NSPCs), neurons differentiated from NSPCs in culture, and MEFs. We also examined X-ray–induced apoptosis in NSPCs and neurons. Here, we demonstrated that DSB repair in neurons is faster than that in MEFs, but similar to that in NSPCs, and that DNA-PKcs expression and DNA-PK activity are higher in both NSPCs and neurons than in MEFs. In addition, we showed that the incidence of X-ray–induced apoptosis is greater in neurons than in NSPCs. This may reflect a difference between neurons and NSPCs in the fidelity of NHEJ or a differential sensitivity to DNA damage other than DSBs.

MATERIALS AND METHODS

Cell culture and neuronal differentiation

Primary striatal neural stem/progenitor cells (NSPCs) were isolated from 14-day embryos (E14) of ICR mice (Japan SLC; Hamamatsu, Japan). The striatums were dissociated with an enzymatic dissociation kit (StemCell Technologies; Vancouver, BC, Canada) according to the manufacturer's instructions. Briefly, the resected striatums were minced and treated with the dissociation solution for 7 min at 37°C, followed by treatment with the inhibition solution. The cell suspension was centrifuged at 1200 rpm for 5 min at room temperature, and the cell pellet was washed twice with the resuspension solution. Then, the cells were cultured in DMEM/Ham's F-12 (Nacalai Tesque; Kyoto, Japan) supplemented with 2% B-27 (Thermo Fisher Scientific; Waltham, MA, USA), 20 ng/ml basic fibroblast growth factor (bFGF) (PeproTech; Rocky Hill, CT, USA), 20 ng/ml epidermal growth factor (EGF) (PeproTech), 2 μg/ml heparin sodium salt and 1% penicillin–streptomycin (Nacalai Tesque), as floating neurospheres at 37°C under humidified 5% CO_2 conditions.

To prepare differentiated neurons, NSPCs were cultured for 48 h on poly-L-ornithine (Sigma-Aldrich; St Louis, MO, USA) -coated dishes in neurobasal medium (Thermo Fisher Scientific) supplemented with 2% B-27, 2 mM L-glutamine and 1% penicillin–streptomycin. During harvest of the striatum, MEFs were also isolated from identical embryos and cultured in minimum essential medium alpha (MEM alpha) (Thermo Fisher) supplemented with 10% fetal bovine serum (FBS) (HyClone; Logan, UT, USA) and 1% penicillin–streptomycin at 37°C under humidified 5% CO_2 conditions.

X-irradiation

Cells were irradiated with 1 Gy or 2 Gy of X-rays by an X-ray machine (OM-B205; Ohmic, Tokyo, Japan) operated at 70 kVp and 5 mA using a 0.5 mm Al filter at room temperature. The dose rate was 0.66 Gy/min.

Western blotting

Neurospheres containing NSPCs were dissociated with accutase (Nacalai Tesque), plated at a density of 5.2×10^5 cells/cm^2 in dishes, and cultured for 3 h. MEFs were dissociated with 0.2% trypsin, plated at a density of 7.3×10^4 cells/cm^2 in dishes, and cultured for 24 h. For differentiated neurons, NSPCs were plated at a density of 5.2×10^5 cells/cm^2 in dishes precoated with poly-L-ornithine (Sigma-Aldrich), and cultured for 48 h for neuronal differentiation in the neurobasal medium described above. At each time point, cells were collected and lysed with lysis buffer containing 50 mM Tris-HCl (pH 8.0), 150 mM NaCl, 0.5% sodium deoxycholate, 0.1% SDS, 1% NP-40, protease inhibitor cocktail (Sigma-Aldrich) and phosphatase inhibitor cocktail (Nacalai Tesque). The lysed cells were incubated on ice for 30 min and centrifuged at 4°C at 14 000 rpm for 10 min. The supernatants were collected and the protein concentration was determined by using a BCA protein assay kit (Thermo Fisher). Protein (20 μg per lane) was separated by SDS-PAGE, and electroblotted to polyvinylidene difluoride membranes (FluoroTrans W; Pall, Washington, NY, USA). The transferred membranes were soaked with blocking buffer containing 50% blocking one (Nacalai Tesque) and 0.1% Tween 20 in TBS at room temperature for 30 min. Blocked membranes were incubated with a primary antibody at 4°C overnight and with a secondary antibody at room temperature for 1 h. The primary antibodies used were anti-βIII-tubulin (Tuj1, 1:1000; Biolegend, San Diego, CA, USA), anti-actin (1:1000; Sigma-Aldrich), anti-cleaved caspase-3 (Asp175) (1:500; Cell Signaling Technology; Danvers, MA, USA), anti-phospho-p53 (Ser15) (1:500; Cell Signaling) and anti-p53 (1C12, 1:500; Cell Signaling), and the secondary antibodies used were goat anti-mouse IgG (H+L) peroxidase conjugated (1:1000; Thermo Fisher) and goat anti-rabbit IgG (H+L) peroxidase conjugated (1:1000; Thermo Fisher). After incubation with Chemi-Lumi One Super (Nacalai Tesque) or Chemi-Lumi One Ultra (Nacalai Tesque) at room temperature for 5 min, proteins were detected by ChemiDoc XRS (Bio-Rad, Hercules, CA, USA). The signal intensity of the bands was quantified by Quantity One (Bio-Rad).

Immunocytostaining

Neurospheres containing NSPCs were dissociated with accutase, plated at a density of 1.0×10^5 cells/cm^2 on coverslips precoated with poly-L-ornithine (Sigma-Aldrich), and cultured for 3 h. MEFs

were dissociated with 0.2% trypsin, plated at a density of 2.1×10^4 cells/cm^2 on coverslips, and cultured for 24 h. For differentiated neurons, NSPCs were plated at a density of 1.0×10^5 cells/cm^2 on coverslips precoated with poly-L-ornithine, and cultured for 48 h for neuronal differentiation in the neurobasal medium described above. At each time point, cells cultured on coverslips were fixed with 4% paraformaldehyde phosphate buffer solution at room temperature for 15 min and permeabilized with 0.5% triton X-100 in PBS (−) on ice for 5 min. Fixed cells were soaked with blocking buffer containing 5% blocking one and 0.1% Tween 20 in PBS (−) at room temperature for 1 h. Blocked cells were incubated with a primary antibody at 4°C overnight and with a secondary antibody at room temperature for 1 h. The primary antibodies used were anti-βIII-tubulin (1:300; Biolegend) and anti-phospo-53BP1 (S25) (1:1000; Bethyl Laboratories, Montgomery, TX, USA). The secondary antibodies used were Alexa Fluor 594 donkey anti-mouse IgG (H + L) (1:100; Thermo Fisher) and Alexa Fluor 488 goat anti-rabbit IgG (H + L) (1:100; Thermo Fisher). The coverslips were mounted by Vectashield mounting medium with DAPI. Fluorescence images were observed by a fluorescence microscope (BX51; Olympus), taken by a digital camera (DP71; Olympus), and processed by DP Manager (Olympus).

Apoptosis assay

Cells cultured on coverslips were fixed with 4% paraformaldehyde phosphate buffer solution (Nacalai Tesque) at room temperature for 15 min and permeabilized with 0.5% Triton X-100 in PBS (−) on ice for 5 min. The coverslips were mounted by Vectashield mounting medium with DAPI (Vector Laboratories, Burlingame, CA, USA). Fluorescence images were observed by a fluorescence microscope, taken by a digital camera, and processed by DP Manager. Pyknotic nuclei were scored as apoptotic cells.

DNA-PK activity assay

Cells were lysed with whole cell extract (WCE) buffer [15] containing 20 mM Hepes (pH 7.6), 450 mM NaCl, 25% glycerol, 0.2 mM EDTA, 0.2 mM DTT, protein inhibitor cocktail and phosphatase inhibitor cocktail. The lysates were incubated on ice for 30 min and centrifuged at 4°C at 14 000 rpm for 10 min. The supernatants were collected and the protein concentration was determined by using protein assay CBB solution (Nacalai Tesque). DNA-PK activity was quantitated by the Signa TECT^R DNA-dependent protein kinase assay system (Promega, Madison, WI, USA). A reaction mixture containing 0.4 mM biotinylated peptide substrate, 1 × DNA-PK reaction buffer, DNA-PK activation buffer (10 μg calf thymus DNA in TE buffer), 0.08 mg/ml BSA, 0.1 mM ATP and 18.5 kBq γ-[^{32}P] ATP (PerkinElmer, Waltham, MA, USA) was preincubated at 30°C for 5 min. The protein supernatant (10 μg) was incubated with the pre-warmed reaction mixture at 30°C for 5 min. Kinase activity was terminated by adding 12.5 μl of termination buffer to each reaction. Subsequently, 10 μl of the reaction mixture from each terminated reaction was spotted onto the biotinylated SAM2^R membrane. The spotted membranes were washed in 2 M NaCl four times, in 2 M NaCl and 1% H_3PO_4 four times and in ultrapure water twice. The radioactivity on the membranes was quantified by a liquid scintillation counter (Tri-carb 2500TR; PerkinElmer).

Statistics

Statistical significance was tested by paired Student's *t*-test. *P*-values <0.05 were considered to indicate statistically significant differences.

RESULTS

Neuronal differentiation from NSPCs in culture

The proportions of NSPCs that expressed Sox2 and Nestin, typical stem cell markers, were 95.8 ± 1.4% and 92.5 ± 1.4%, respectively, indicating that NSPCs possessed the characteristics of neural stem cells. To obtain differentiated neurons from NSPCs, we cultured NSPCs in neurobasal medium for 48 h *in vitro*, and confirmed that NSPCs differentiated into neurons as shown in Fig. 1. Along with differentiation from NSPCs, neurons gradually changed morphology, from a round shape to a spindle shape, and finally took on a neuron-like morphology with outgrowing neurites (Fig. 1A) and expressed βIII-tubulin, a young post-mitotic neuronal marker (Fig. 1B and C). The expression of βIII-tubulin in neurons was significantly increased to 13-fold that in NSPCs. The expression of βIII-tubulin was confirmed by immunocytostaining, as shown in Fig. 1D. The population of βIII-tubulin–positive cells in neurons increased significantly compared with that in NSPCs (NSPCs, 1.4 ± 0.6%; neurons, 82.4 ± 1.8%) (Fig. 1E). These results indicate that NSPCs differentiate into neurons in the neurobasal medium over 48 h of culture. In contrast, βIII-tubulin–positive cells were not detected in MEFs (Fig. 1D and E). However, the incidence of apoptosis detected by pyknotic nuclei [16, 17] during differentiation was significantly increased in neurons compared with in NSPCs (NSPCs, 1.6 ± 0.2%; neurons, 37.0 ± 0.8%) (Fig. 1F). We confirmed that apoptosis was induced to a similar extent (36.8%) during differentiation as a subG1 fraction by flow cytometry.

Time-dependent appearance of apoptotic cells during differentiation from NSPCs into neurons in culture

We then investigated the association between neuronal differentiation and the incidence of apoptosis during the first 48 h in culture. The morphology of NSPCs was changed during neuronal differentiation in culture (Fig. 2A). Proteolytically cleaved caspase-3, a marker of apoptosis, increased time dependently up until 12 h and then decreased gradually up until 48 h (Fig. 2B, top panel). Because the tumor suppressor p53, which is phosphorylated at Ser18 (corresponding to Ser15 of human p53) by ataxia telangiectasia mutated (ATM) protein in response to DNA damage [18], might play a critical role in apoptosis induction, we examined the levels of phosphorylated p53 (p-p53) and p53. The p-p53 (Ser18) and p53 gradually accumulated during neuronal differentiation in culture for up to 6 h and then decreased gradually up until 48 h. (Fig. 2B, second and third panels). As expected, the increase in βIII-tubulin expression was concomitant with the morphological change from NSPCs to neurons (Fig. 2B, fourth panel). Considering the possibility that the induction of cleaved caspase-3 does not always indicate

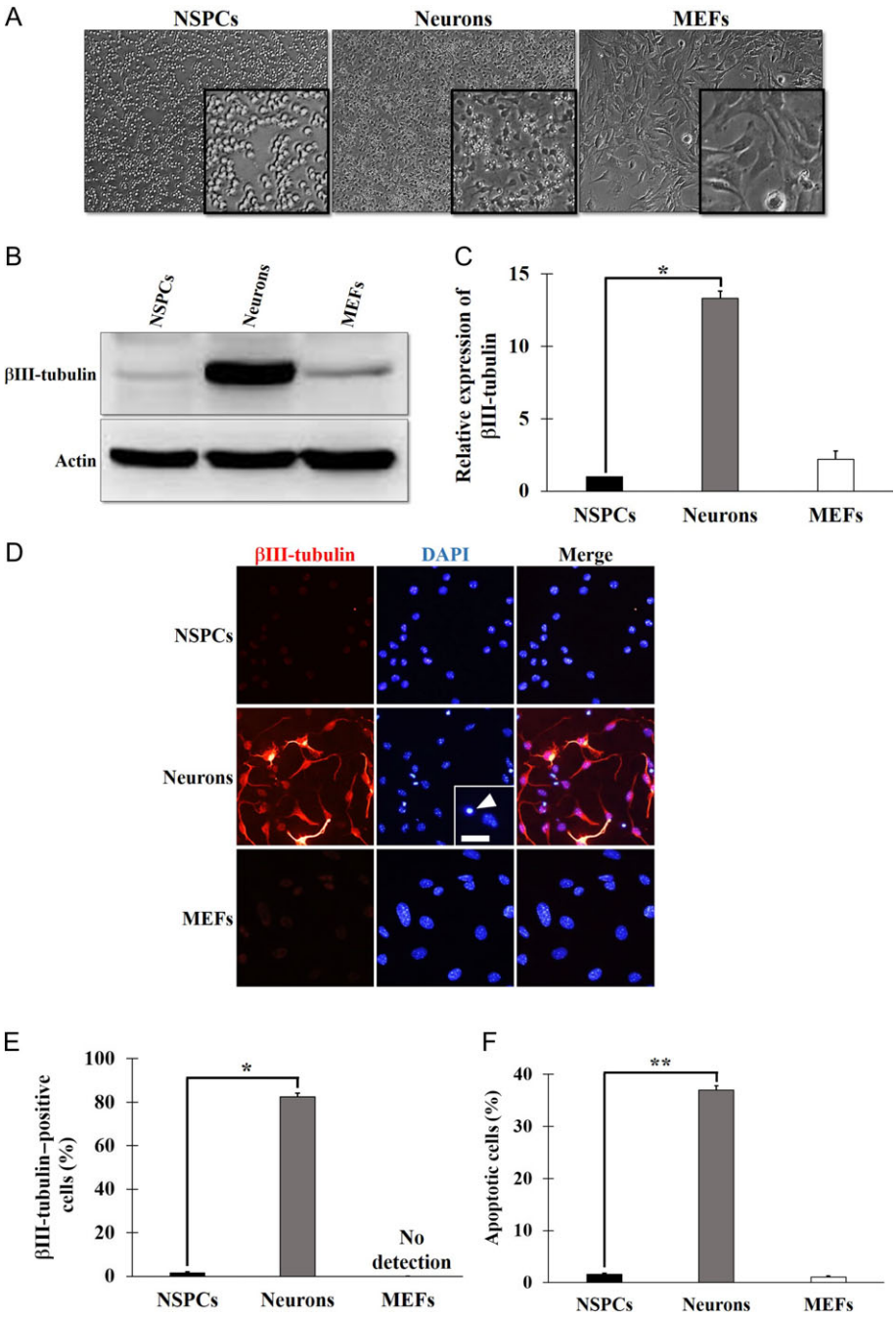

Fig. 1. Neuronal differentiation from neural stem/progenitor cells (NSPCs) in culture. (A) Bright-field images of NSPCs, neurons differentiated from NSPCs in culture for 48 h, and mouse embryonic fibroblasts (MEFs). The insets are enlarged images of the indicated cells. (B) Western blotting with βIII-tubulin. Lysates of NSPCs, neurons and MEFs were subjected to SDS-PAGE, and βIII-tubulin and actin were detected with anti-βIII-tubulin and anti-actin antibodies. Actin was used as a loading control. (C) Quantification of the βIII-tubulin expression. The signal intensity of the bands corresponding to βIII-tubulin was normalized to that of the actin. The values of three independent experiments were represented as the means ± S.E.M. *$P = 0.0004$ by paired Student's *t*-test. (D) Immunocytostaining of the βIII-tubulin. NSPCs, neurons, and MEFs were immunocytostained with anti-βIII-tubulin (red) antibody. Nuclei were counterstained with DAPI (blue). The inset is an enlarged image. The arrowhead shows a pyknotic nucleus, indicating apoptosis. Scale bar, 50 μm. (E, F) Quantification of βIII-tubulin–positive cells (E) and apoptotic cells (F). Nine fields per experiment were analyzed. The values of three independent experiments are represented as the means ± S.E.M. *$P = 0.0013$ (E), **$P = 0.0007$ (F) by paired Student's *t*-test.

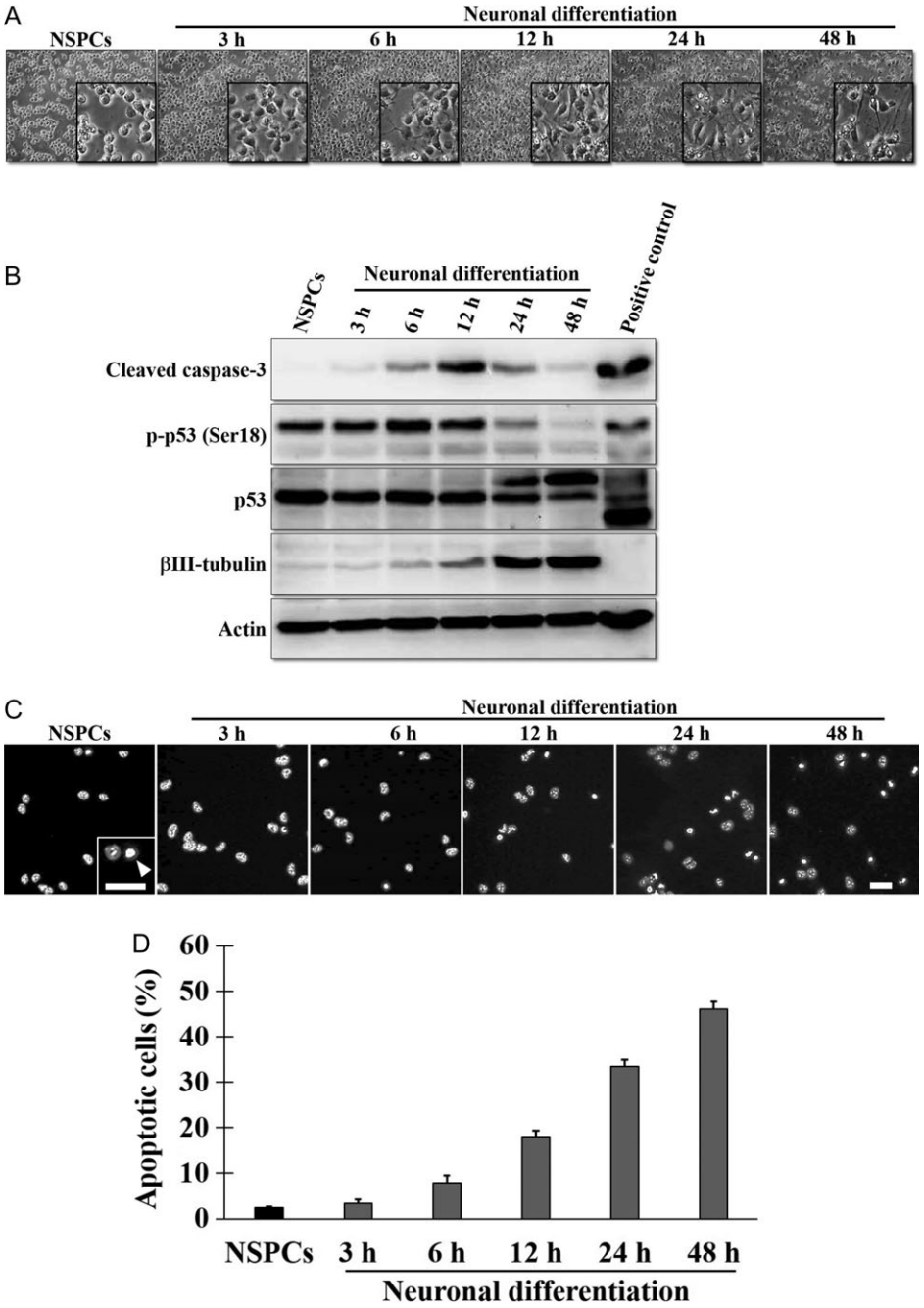

Fig. 2. Time-dependent appearance of apoptotic cells during differentiation from NSPCs to neurons in culture. (A) Bright-field images of NSPCs and neurons at the indicated time points during neuronal differentiation in culture. The insets are enlarged images of the cells. (B) Western blotting of the cleaved caspase-3, the phosphorylated p53 at Ser18 (p-p53 (Ser18)), the p53 and the βIII-tubulin. Lysates of NSPCs and neurons differentiated for 3 h to 48 h in culture were subjected to SDS-PAGE, and the indicated proteins were detected with anti-cleaved caspase-3, anti-p-p53 (Ser18), anti-p53, anti-βIII-tubulin and anti-actin antibodies. Mouse lymphocytes irradiated with 6 Gy of X-rays were used as a positive control for apoptosis. (C) Immunofluorescence images of NSPCs and neurons differentiated for 3 h to 48 h in culture. Nuclei were stained with DAPI (gray). The inset is an enlarged image. The arrowhead shows a pyknotic nucleus, indicating apoptosis. Scale bar, 50 μm. (D) Quantification of apoptotic cells. Sixteen fields per experiment were analyzed. The values of three independent experiments are represented as the means ± S.E.M.

apoptosis during neuronal differentiation [19], we then determined the incidence of apoptosis during neuronal differentiation in culture by scoring pyknotic nuclei (Fig. 2C and D). The results indicated that apoptosis increased time dependently during differentiation from NSPCs to neurons in culture. Collectively, the results shown in Fig. 2B indicated that the increase in apoptosis was not dependent on the accumulation of p-p53 or p53, indicating that p53-independent apoptosis occurred time dependently during neuronal differentiation in culture.

Faster DSB repair in NSPCs and neurons than in MEFs

To examine whether neurons can repair DSBs more efficiently than NSPCs and MEFs, we examined the kinetics of DSB repair from 10 min to 12 h post-irradiation in neurons, NSPCs and MEFs by detecting the foci of phosphorylated 53BP1 at Ser25 (p-53BP1) (Fig. 3). The kinetics of DSB repair was represented as the relative ratio of p-53BP1 foci per cell at a given time to that at 10 min post-irradiation, as shown in Fig. 3B, because the numbers of p-53BP1 foci per cell at 10 min post-irradiation in both NSPCs and neurons (10.5 ± 0.5 and 14.7 ± 0.6 in average, respectively) were less than those in MEFs (35.3 ± 0.6 in average), possibly reflecting the thickness of the sample cells. In neurons and NSPCs, the relative number of DSBs per cell decreased time dependently from 10 min to 12 h post-irradiation (Fig. 3A and B). In contrast, the relative number of DSBs per cell in MEFs was constant from 10 min to 1 h and then decreased time dependently from 1 h to 12 h. These results indicated that DSB repair for up to 6 h post-irradiation in neurons and NSPCs was significantly faster than that in MEFs, and that the DSB repair kinetics of neurons was similar to that of NSPCs.

Higher expression of DNA-PKcs and DNA-PK activity in NSPCs and neurons than in MEFs

As neurons are post-mitotic cells, they repair DSBs by NHEJ [2, 8, 20], and DNA-PK plays an essential role in this process [21, 22]. To examine why the DSB repair in NSPCs and neurons was faster than that in MEFs, we determined the expression levels of DNA-PKcs in NSPCs and neurons and compared them with the expression level in MEFs. The expression level of DNA-PKcs in NSPCs and neurons was significantly higher than that in MEFs, whereas no significant difference was seen between the level in NSPCs and neurons (Fig. 4A and B). We then examined temporal changes in the expression of DNA-PKcs from 1 h to 12 h post-irradiation. No significant change was observed in any of the cells tested (Fig. 4C and D). Next, to determine whether the expression of DNA-PKcs was correlated with DNA-PK activity, we determined the levels of DNA-PK activity in NSPCs, neurons and MEFs (Fig. 4E). DNA-PK activity was measured by the ability to phosphorylate a substrate derived from the human p53 peptides. The DNA-PK activity levels of NSPCs and neurons were almost 2-fold higher than the level in MEFs, and this trend in DNA-PK activity was not affected by X-irradiation (Fig. 4E). These results indicated that NSPCs and neurons have higher DNA-PK activity for promoting DSB repair compared with MEFs.

Higher incidence of X-ray–induced apoptosis in neurons than in NSPCs

As shown in Fig. 3, DSB repair in NSPCs and neurons was faster than that in MEFs. However, we cannot exclude the possibility that the faster DSB repair kinetics was due to the higher incidence of apoptosis, which may have eliminated heavily damaged cells in NSPCs and neurons. To elucidate the incidence of apoptosis induced by X-irradiation, we determined the temporal changes in the accumulation of cleaved caspase-3 from 10 min to 12 h post-irradiation in NSPCs, neurons and MEFs (Fig. 5A). In NSPCs and MEFs, cleaved caspase-3 was not accumulated under control conditions, whereas a low level of accumulation was observed in neurons (Fig. 5A), indicating that apoptosis emerged in unirradiated neurons, as shown in Fig. 1F. Moreover, in NSPCs and neurons, but not in MEFs, the accumulation of cleaved caspase-3 increased at 3 h, peaked at 6 h, and decreased at 12 h (Fig. 5A, top panel, 5th panel). This result, together with the result in Fig. 3B, indicated that the apoptosis induction was initiated at 3 h post-irradiation, at which time point most (three-quarters) of DSBs were repaired in both NSPCs and neurons, suggesting that the fast DSB repair kinetics were not due to the elimination of damaged cells by apoptosis.

We also examined whether the accumulation of cleaved caspase-3 was dependent on the expression and the phosphorylation of p53. In all cells examined, both the p53 and the p-p53 accumulated time dependently post-irradiation, indicating that apoptosis in NSPCs and neurons emerged due to the p53-dependent DNA damage response. We further determined the incidence of apoptosis in NSPCs, neurons and MEFs by scoring pyknotic nuclei at 6 h post-irradiation, in which the accumulation of cleaved caspase-3 showed a peak (Fig. 5B and C). Because the rate of spontaneous incidence of apoptosis was higher in neurons than in NSPCs and MEFs, the X-ray–induced incidence of apoptosis was calculated as the total incidence minus the spontaneous incidence. The incidence of apoptosis in neurons exposed to 1 Gy of X-rays was significantly higher than that in NSPCs (NSPCs, 8.7 ± 1.3%; neurons, 25.4 ± 2.8%), and a similar result was obtained with 2 Gy of X-rays (NSPCs, 12.2 ± 1.4%; neurons, 34.8 ± 2.2%). Apoptosis was not induced by either 1 or 2 Gy X-irradiation in MEFs.

DISCUSSION

In the present study, we examined the DSB repair kinetics in X-ray–induced DSBs in NSPCs, neurons differentiated from NSPCs in culture, and MEFs derived from the same littermates, and demonstrated that DSB repair in neurons was faster than that in MEFs, but similar to that in NSPCs (Fig. 3B). In addition, we found higher levels of DNA-PKcs expression and DNA-PK activity in neurons and NSPCs than in MEFs (Fig. 4B and E). These findings indicate that NHEJ activity in neurons and NSPCs was enhanced compared with that in MEFs. Neural cells such as NSPCs and neurons can generate more ROS than other cells due to the high consumption of oxygen in the brain [5, 6]. DSBs are the most lethal form among a variety of DNA damages induced by ROS. Thus, we speculated that neural cells have the ability to repair DSBs more quickly than other cells in order to survive for a long time in an environment where DSBs are readily generated. This notion is further supported by the fact that fast DSB repair is also observed in astrocytes, which are also differentiated from NSPCs [23].

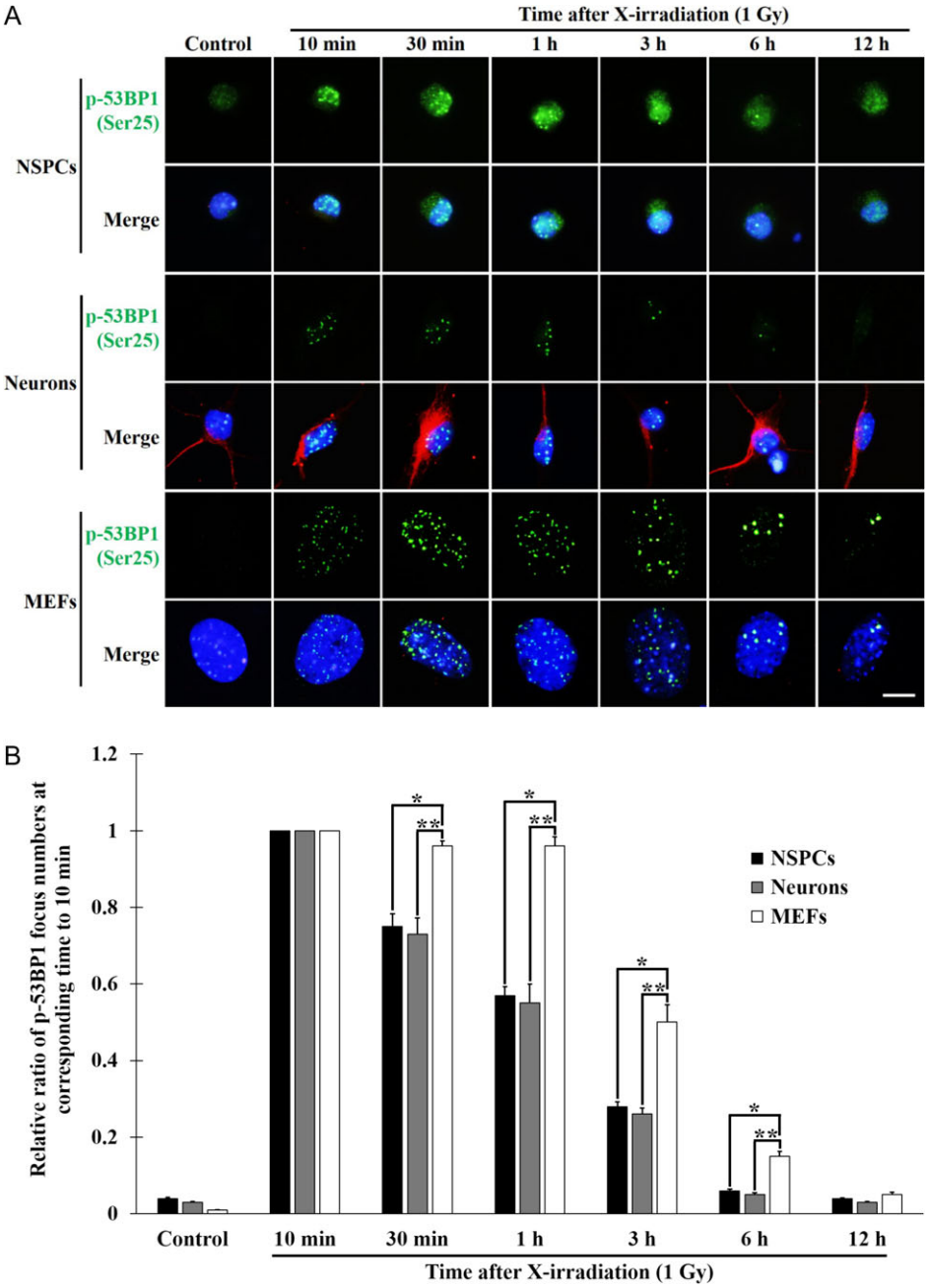

Fig. 3. Repair kinetics of DNA double-strand breaks in NSPCs, neurons and MEFs. (A) Immunocytostaining of the phosphorylated 53BP1 at Ser25 (p-53PB1 (Ser25)) and the βIII-tubulin. NSPCs, neurons and MEFs cultured for the indicated times post-irradiation (1 Gy) were immunocytostained with anti-p-53BP1 (Ser25) (green) and anti-βIII-tubulin (red) antibodies. Nuclei were counterstained with DAPI (blue). Scale bar, 20 μm. (B) The relative ratio of p-53BP1 (Ser25) foci. In neurons, the p-53BP1 (Ser25) foci in the βIII-tubulin–positive cells were counted and represented as the relative ratio of the focus number at the corresponding time to that at 10 min post-irradiation. Two hundred cells per experiment were analyzed. The relative values of three independent experiments were represented as the means ± S.E.M. *$P = 0.0209$, **$P = 0.0332$ (30 min); *$P = 0.0028$, **$P = 0.0164$ (1 h); *$P = 0.003$, **$P = 0.0064$ (3 h); and *$P = 0.0015$, **$P = 0.0006$ (6 h); all by paired Student's *t*-test.

In general, it is well known that immature cells during developmental stages are more sensitive to ionizing radiation than mature cells, suggesting that NSPCs should show a higher sensitivity to X-irradiation than neurons. However, we found that X-irradiation induced more apoptotic cells in neurons than in NSPCs, regardless of the similar DSB repair kinetics. In Fig. 3, most (three-quarters)

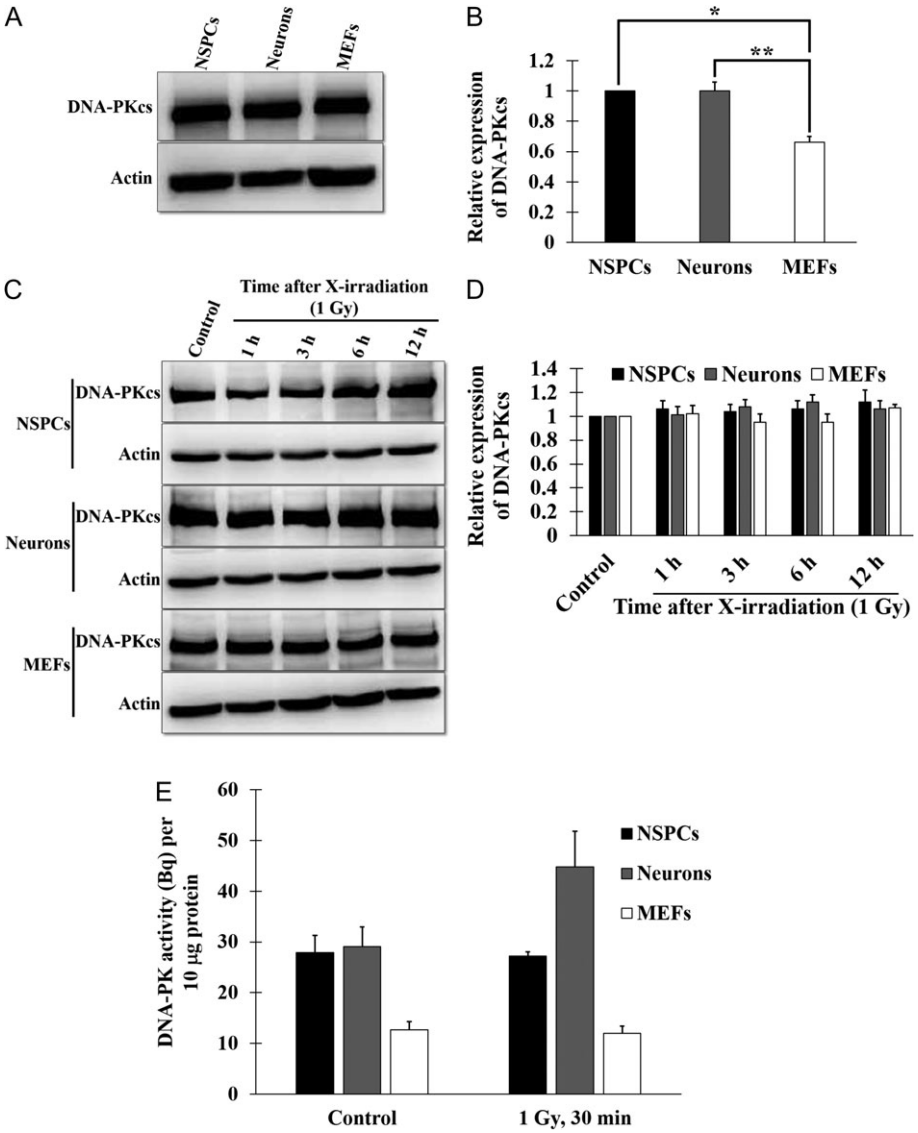

Fig. 4. The expression of DNA-PKcs and DNA-PK activity in NSPCs, neurons and MEFs. (A, C) Western blotting of DNA-PKcs. Lysates of NSPCs, neurons, MEFs (A), and the indicated cells cultured for the indicated times post-irradiation (1 Gy) (C) were subjected to SDS-PAGE, and the DNA-PKcs and the actin were detected with anti-DNA-PKcs and anti-actin antibodies. (B, D) Quantification of the DNA-PKcs expression. The signal intensity of the bands corresponding to the DNA-PKcs was normalized to that of the actin. (E) DNA-PK activity in NSPCs, neurons and MEFs. Lysates of NSPCs, neurons and MEFs cultured for 30 min post-irradiation (1 Gy) were used for measuring the ability to phosphorylate a substrate derived from the human p53 peptides. The values of three independent experiments are represented as the means ± S.E.M. *$P = 0.0114$, **$P = 0.0185$ (B) by paired Student's *t*-test.

of DSBs were diminished by 3 h post-irradiation, and the majority of DSBs were repaired by 6 h in both NSPCs and neurons. Therefore, the fact that more apoptotic cells were induced in neurons than in NSPCs at 6 h post-irradiation, as shown in Fig. 5C, cannot be explained by the difference in the number of residual DSBs in neurons and NSPCs. We considered two possible explanations. The first is that the errors leading to apoptosis occur due to a lower fidelity of NHEJ in neurons. This speculation is partly supported by the finding that the fidelity of NHEJ is lower in astrocytes compared with that in neural progenitors differentiated from human embryonic stem cells [24]. The second possibility we considered is that not only DSBs but also other DNA lesions are responsible for the induction of apoptosis. Ionizing radiation induces a variety of DNA lesions, including base lesions that are repaired by base excision repair (BER) [25]. The ability to repair DNA, including via BER, is attenuated during differentiation in most cell types [26–28]. This suggests that more base lesions can be accumulated in differentiated cells such as neurons than in NSPCs. Moreover, 8-oxoguanine, one

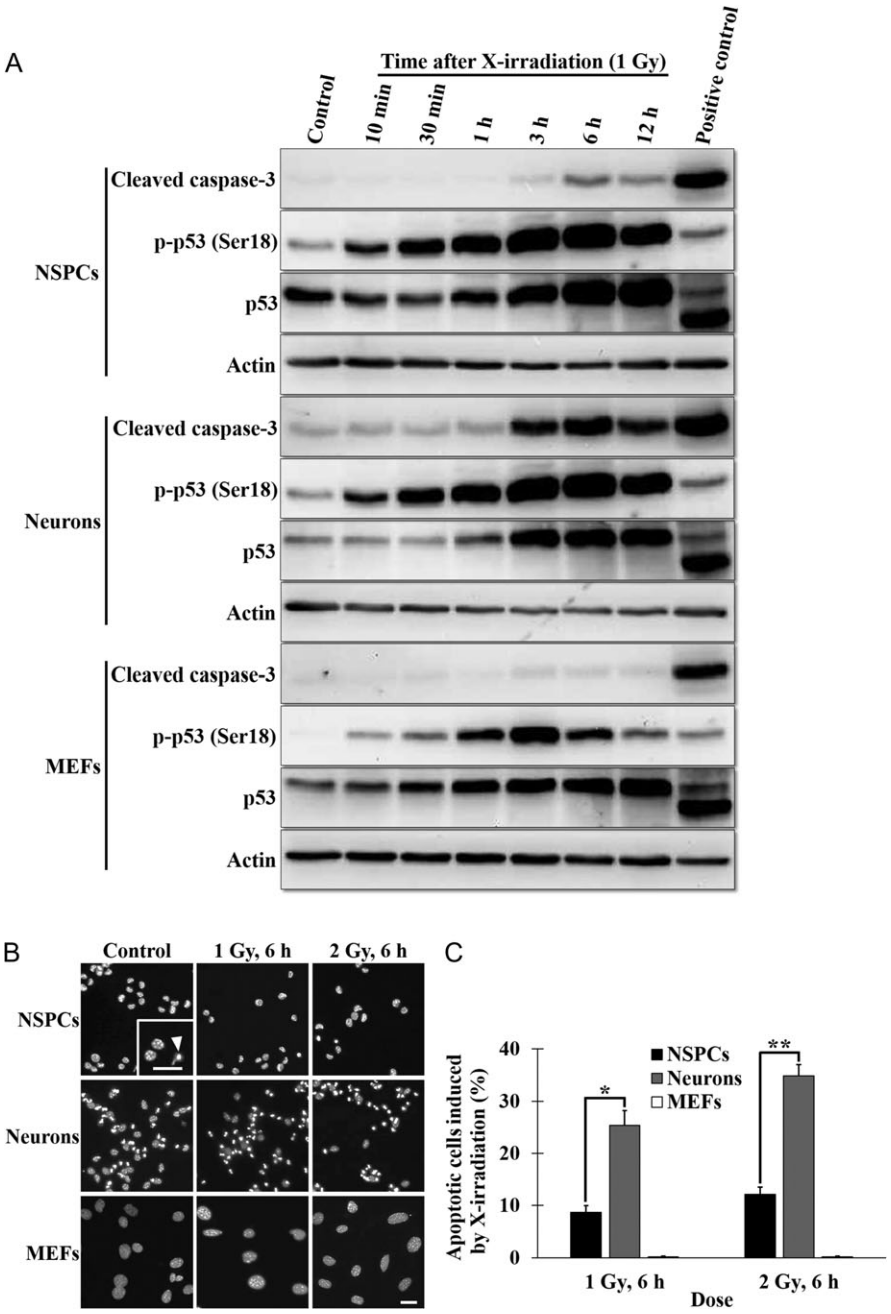

Fig. 5. The incidence of apoptosis induced by X-irradiation in NSPCs and neurons. (A) Western blotting of the cleaved caspase-3, the p-p53 (Ser18) and the p53. Lysates of NSPCs, neurons and MEFs cultured for the indicated times post-irradiation (1 Gy) were subjected to SDS-PAGE, and the expressions of the indicated proteins were detected with anti-cleaved caspase-3, anti-p-p53 (Ser18), anti-p53 and anti-actin antibodies. Mouse lymphocytes cultured for 6 h after X-irradiation (6 Gy) were used as a positive control for apoptosis. (B) Immunofluorescence images of NSPCs, neurons and MEFs. Nuclei of NSPCs, neurons and MEFs cultured for 6 h after 1 Gy or 2 Gy of X-rays were stained with DAPI (gray). The inset is an enlarged image. The arrowhead shows a pyknotic nucleus, indicating apoptosis. Scale bar, 50 μm. (C) Quantification of apoptotic cells. Sixteen fields per experiment were analyzed. The values of three independent experiments are represented as the means ± S.E.M. *$P = 0.041$, **$P = 0.0167$ by paired Student's *t*-test.

of the major base lesions, accumulates in patients with neurodegenerative diseases such as Alzheimer's and Parkinson's diseases [29, 30]. These findings suggest that the difference in DNA repair ability in response to DNA damage other than DSBs is responsible for the differential incidence of apoptosis between neurons and NSPCs. However, whether there is a difference in the number of base lesions persisting in neurons and NSPCs at the time that apoptosis emerges post-irradiation remained to be elucidated in the present study.

As shown in Fig. 2B, p53 was phosphorylated and stabilized in unirradiated NSPCs. This slight accumulation of p53 was probably a p53 response to culture conditions in which NSPCs were forced to differentiate into neurons in neurobasal medium. During the differentiation from NSPCs into neurons in culture, p-p53 and p53 gradually accumulated for up to 6 h and then decreased until 48 h, and the cleaved caspase-3 accumulated until 12 h and then decreased until 48 h. In a previous study, it was reported that endogenous caspase-3 activity was elevated during neuronal differentiation and that the inhibition of caspase-3 activity did not affect apoptosis but delayed neuronal differentiation [19]. Therefore, we speculated that the accumulation of the cleaved caspase-3, the p-p53 and the p53 was engendered in association with neuronal differentiation, but not with the incidence of apoptosis. In contrast to this, as shown in Fig. 5A, the time-dependent accumulation of the cleaved caspase-3, the p-p53 and the p53 post-irradiation in neurons suggested that the apoptosis observed at 6 h post-irradiation (Fig. 5B and C) was induced by the p53-dependent DNA damage response. Therefore, the present study demonstrated two distinct pathways of apoptosis in neurons: p53-independent apoptosis engendered during differentiation from NSPCs to neurons and p53-dependent apoptosis engendered as part of the DNA damage response induced by X-irradiation.

Recently, cranial irradiation has been reported to cause symptoms similar to Alzheimer's disease, raising serious concerns about radiation therapy and the risks of impairments of cognitive function and spatial learning [31, 32]. To clarify the mechanism for the cognitive impairment induced by radiation, it is crucial to understand the pathway of radiation-induced neuronal death. In the present study, we investigated the DSB repair and cell death induced by ionizing radiation in neurons differentiated from NSPCs, and demonstrated that DSB repair in neurons and NSPCs was faster than that in MEFs, and that more apoptotic cells were induced in neurons than in NSPCs. However, we cannot exclude the possibility that the culture conditions in which the NSPCs were forced to differentiate into neurons could make neurons more susceptible to radiation-induced apoptosis. In neuronal differentiation in culture, the majority of NSPCs differentiate into glial cells, not neurons. In relation to this, treatment of NSPCs with some chemicals such as cell cycle blockers has been reported to improve neuronal differentiation without enhancement of apoptosis [33, 34]. Nevertheless, the ratios of differentiation into neurons in the calibrated medium remain low (<30%). Although the cell culture system we adopted in the present study showed technical limitations in terms of inducing a high fraction of apoptosis (Fig. 1F), we suggest that this system allows efficient neuronal differentiation (Fig. 1E) and thus is practically useful for investigating the repair kinetics of DSBs in neurons.

CONFLICT OF INTEREST

The authors declare that there are no conflicts of interest.

FUNDING

This work was supported by a Grant-in-Aid for Challenging Exploratory Research from the Japan Society for the Promotion of Science (JSPS) [grant number JP 16K12599].

REFERENCES

1. Bredesen DE, Rao RV, Mehlen P. Cell death in the nervous system. *Nature* 2006;443:796–802.
2. Iyama T, Wilson DM III. DNA repair mechanisms in dividing and non-dividing cells. *DNA Repair (Amst)* 2013;12:620–36.
3. Suberbielle E, Sanchez PE, Kravitz AV et al. Physiologic brain activity causes DNA double-strand breaks in neurons, with exacerbation by amyloid-β. *Nat Neurosci* 2013;16:613–21.
4. Enokida Y, Tamura T, Ito H et al. Mutant huntingtin impairs Ku70-mediated DNA repair. *J Cell Biol* 2010;189:425–43.
5. Floyd RA, Hensley K. Oxidative stress in brain aging. Implications for therapeutics of neurodegenerative diseases. *Neurobiol Aging* 2002;5:795–807.
6. Brasnjevic I, Hof PR, Steinbusch HW et al. Accumulation of nuclear DNA damage or neuron loss: molecular basis for a new approach to understanding selective neuronal vulnerability in neurodegenerative diseases. *DNA Repair (Amst)* 2008;7:1087–97.
7. Madabhushi R, Gao F, Pfenning AR et al. Activity-induced DNA breaks govern the expression of neuronal early-response genes. *Cell* 2015;161:1592–605.
8. Shibata A, Jeggo PA. DNA double-strand break repair in a cellular context. *Clin Oncol* 2014;26:243–9.
9. Ochi T, Blackford AN, Coates J et al. PAXX, a paralog of XRCC4 and XLF, interacts with Ku to promote DNA double-strand repair. *Science* 2015;347:185–8.
10. Xing M, Yang M, Huo W et al. Interactome analysis identifies a new paralogue of XRCC4 in non-homologous end joining DNA repair pathway. *Nat Commun* 2015;6:6233.
11. Craxton A, Somers J, Munner D et al. XLF (C9orf142) is a new component of mammalian DNA double-strand break repair. *Cell Death Diff* 2015;22:890–7.
12. Jiang W, Crowe JL, Liu X et al. Differential phosphorylation of DNA-PKcs regulates the interplay between end-processing and end-ligation during nonhomologous end-joining. *Mol Cell* 2015;58:172–85.
13. Barnes DE, Stamp G, Rosewell I et al. Targeted disruption of the gene encoding DNA ligase IV leads to lethality in embryonic mice. *Curr Biol* 1998;8:1395–8.
14. Gao Y, Sun Y, Frank KM et al. A critical role for DNA end-joining proteins in both lymphogenesis and neurogenesis. *Cell* 1998;95:891–902.
15. Cardinale A, Racaniello M, Saladini S et al. Sublethal doses of β-amyloid peptide abrogate DNA-dependent protein kinase activity. *J Biol Chem* 2012;287:2618–31.

16. Hasegawa K, Yoshikawa K. Necdin regulates p53 acetylation via sirtuin1 to modulate DNA damage response in cortical neurons. *J Neurosci* 2008;28:8772–84.
17. Rousseau L, Etienne O, Roque T et al. *In vivo* importance of homologous recombination DNA repair for mouse neural stem and progenitor cells. *PloS One* 2012;7:e37194.
18. Kruse JP, Gu W. Modes of p53 regulation. *Cell* 2009;137:609–22.
19. Fernando P, Brunetts S, Megeney LA. Neural stem cell differentiation is dependent upon endogenous caspase 3 activity. *FASEB J* 2005;19:1671–3.
20. Beucher A, Birraux J, Tchouandong L et al. ATM and Artemis promote homologous recombination of radiation-induced DNA double strand breaks in G2. *EMBO J* 2009;28:3413–27.
21. Riballo E, Kühne M, Rief N et al. A pathway of double-strand break rejoining dependent upon ATM, Artemis, and proteins loading to γ-H2AX foci. *Mol Cell* 2004;16:715–24.
22. Goodarzi AA, Yu Y, Riballo E et al. DNA-PK autophosphorylation facilitates Artemis endonuclease activity. *EMBO J* 2006;25:3880–9.
23. Gobbel GT, Bellinzona M, Vogt AR et al. Response of postmitotic neurons to X-irradiation: implications for the role of DNA damage in neuronal apoptosis. *J Neurosci* 1998;18:147–55.
24. Adams BR, Hawkins AJ, Povirk LF et al. ATM-independent, high-fidelity nonhomologous end joining predominates in human embryonic stem cells. *Aging (Albany NY)* 2010;2:582–96.
25. Shikazono N, Noguchi M, Fujii K et al. The yield, processing, and biological consequences of clustered DNA damage induced by ionizing radiation. *J Radiat Res* 2009;50:27–36.
26. Nouspikel T, Hanawalt PC. Terminally differentiated human neurons repair transcribed genes but display attenuated global DNA repair and modulation of repair gene expression. *Mol Cell Biol* 2000;20:1562–70.
27. Narciso L, Fortini P, Pajalunga D et al. Terminally differentiated muscle cells are defective in base excision DNA repair and hypersensitive to oxygen injury. *Proc Natl Acad Sci U S A* 2007; 104:17010–5.
28. Fortini P, Ferretti C, Dogliotti E. The response to DNA damage during differentiation: pathways and consequences. *Mutat Res* 2013;743–4:160–8.
29. Shimura-Miura H, Hattori N, Kang D et al. Increased 8-oxo-dGTPase in the mitochondria of substantia nigral neurons in Parkinson's disease. *Ann Neurol* 1999;46:920–4.
30. Nunomura A, Perry G, Aliev G et al. Oxidative damage is the earliest event in Alzheimer disease. *J Neuropathol Exp Neurol* 2001;60:759–67.
31. Raber J, Fan Y, Matsumori Y et al. Irradiation attenuates neurogenesis and exacerbates ischemia-induced deficits. *Ann Neurol* 2004;55:381–9.
32. Cherry JD, Liu B, Frost JL et al. Galactic cosmic radiation leads to cognitive impairment and increased Aβ plaque accumulation in a mouse model of Alzheimer's disease. *PloS One* 2012;7: e53275.
33. Kim HJ, Hida H, Jung CG et al. Treatment with deferoxamine increases neurons from neural stem/progenitor cells. *Brain Res* 2006;1092:1–15.
34. Misumi S, Kim TS, Jung CG et al. Enhanced neurogenesis from neural progenitor cells with G1/S-phase cell cycle arrest is mediated by transforming growth factor beta1. *Eur J Neurosci* 2008;28:1049–59.